



RESEARCH ARTICLE

Effect of Heat Flow Condition in Analysis of Electron Beam Welding

***Suresh Akella¹, Harinadh Vemanaboina¹, Ramesh Kumar Buddu²**

¹Sreyas Institute of Engineering & Technology, Hyderabad-500068, India.

²FRMDC Division, Institute for Plasma Research, Bhat, Gandhinagar-382428, India.

Received- 8 October 2016, Revised- 16 November 2016, Accepted- 19 December 2016, Published- 29 December 2016

ABSTRACT

Electron Beam welding (EBW) is modeled using a basic Kaplan keyhole formation as in laser beam welding. As high penetration depth to width ratios can be obtained in this process, researchers and engineers are working to enhance this vacuum based technology of component joining. This welding technique has several applications in fusion reactor fabrication of various components like vacuum vessel and test blanket modules with different types of steels. This study is focused on simulating and modeling EBW in terms of the heat flux flow with surface heat on bead area in the form of Gaussian distribution. When the beam forms keyhole plasma, the heat flow conducted to the base metal is modeled as a frustum distribution. Unlike laser beam welding, in EBW, a portion of the heat would leave out to ambience through the lower end of the bead, where this amount of heat is to be apportioned. Heat flow mechanism is calculated using Peclet number from where the empirical formulae power distribution is determined. Peclet number variation is calculated as a function of radial distance, penetration depth and distance from wall. The values obtained may not be directly used in analysis but a correlation is obtained which assists in formulating a finite element analysis. The welding process is evaluated using temperature profile distributions in Weld Zone (WZ) and Heat Affected Zone (HAZ) using Ansys software. SS304 weld material is used and temperature dependent thermal and structural properties are considered. The output obtained is the thermal isotherms around the weld to estimate the surface heat flux distribution on the surface and through the keyhole. The scope of applications where the heat flow distributed in % contribution would provide guidance in structural joints as in nuclear reactor fabrication applications.

Keywords: EBW, Peclet number, Heat power distribution, Ansys simulation.

1. INTRODUCTION

Electron beam welding is widely used in technological applications where the structural integrity is highly demanding in terms of very low distortions and low heat affected zone with good mechanical properties. Electron beam technique employs high power density supply to the localized portion of the structure with fine control and produces low residual stress with narrow weld bead formation. Recent applications of the structural components in the nuclear sector like fusion and fission reactors have shown keen demand in the electron beam applications due to the stringent working conditions, thermo-mechanical specifications and integrity of the

complex structures [1, 2]. In spite of the expensive technique, the application is explored for demonstrative purposes as well as the final engineered products. Analysing the state of the residual stress and temperature profile at several stages will be very helpful to design the product features like the influential characteristics, metallurgical properties and the liquid melt pool behaviour during solidification with the material properties. It is a challenging task to implement the conditions such as the high temperature properties, structural status and the models. This paper is focussed on the analysis of the electron beam weld process pertaining to SS 304 L plates using Peclet number analysis where the

*Corresponding author. Tel.: +919849628282

Email address: s4akella@gmail.com (S.Akella)

<https://dx.doi.org/10.24951/sreyasijst.org/2016011001>

Double blind peer review under responsibility of Sreyas Publications

ISSN© 2016 Sreyas Publications by Sreyas Institute of Engineering and Technology. This is an open access article under the CC BY-NC-ND license (<http://creativecommons.org/licenses/by-nc-nd/4.0/>).

empirical thermal heat conduction to convection ratio is performed. Also as observed in the similar power density application like laser beam welding, the differences are identified and applied to the analysis, based on the thermal isotherms with the heat source input models such as Gaussian beam source and frustum type heat source models [3-5]. The electron beam profile during the plasma key hole spread distribution is analysed with equivalent full Gaussian, partial frustum and Gaussian source heat flow models. The results are analysed in terms of thermal distribution towards the weld and heat affected zone planes.

In EBW, free electrons of charge $1.6 \times 10^{-19} \text{ C}$ are accelerated using electric field and focused on joining metal space as shown in figure A1. Higher the electron beam weld, higher is the metal penetration and material melting. A vacuum space is created around the surface to avoid beam distortion and dissipation and to maintain focussing. In the presence of air or gas, collision with gas molecules would create ionization of molecules and destroy cathode. Vacuum prevents chemical corrosion and eliminates blow holes and bubbles that might happen even when inert gases are used as in LBW. Just like LBW the focused beam restricts fusion zone area and hence has very high power density, up to 10^{10} W/m^2 where area is of 10^9 m^2 . Initially, the beams transfer heat to the surface of fusion zone. When heat gets accumulated, it is penetrated to few microns depth and the molten metal is exposed to severe heat vaporisation and gradually a vapour cover is formed over the entrapped beams. Keyhole formation occurs as how in the LBW process and there will be more efficient usage of beam energy to be used in the fusion process. In this study, the contribution of heat on the surface and the inner keyhole is distributed and analysed by the use of Peclet number. Different ratios of surface to keyhole power distribution are noted from the estimated power and its effect on temperature, distortion and residual stresses are determined.

2. FORMATION AND SIMULATION OF WELDING PROCESS

The heat energy equations are referenced in many articles including an isotropic, conductive material having equal

coefficient of conductivity, $k_x, k_y, k_z (\text{W/mK})$ in all three chosen orthogonal co-ordinates. Equation (2.1) gives the heat energy in the weld area with temperature ($T(\text{K})$) obtained both in spatial, $x, y, z (\text{m})$ and temporal ($t (\text{sec})$), terms. $Q (\text{W/m}^3 \text{ or } \text{J/m}^3 \text{ s})$ is the net heat from the input and the losses in the form of convection and radiation. Density ($\rho (\text{kg/m}^3)$) and specific heat capacity (c), give the right hand terms of how much heat is retained with respect to time in the material and how much is taken away with the velocity of welding ($v (\text{m/s})$). The essential boundary conditions given throughout the body are $T_0(x, y, z, 0)$ at time zero or at the starting of the weld. In addition, the natural boundary conditions have to be applied that consist of normal conduction ($K_n \frac{\delta T}{\delta n}$) heat flux (q), convection ($h (T - T_0)$) and the radiation term ($\sigma \epsilon (T^4 - T_0^4)$).

$$kx \frac{\delta^2 T}{\delta x^2} + ky \frac{\delta^2 T}{\delta y^2} + kz \frac{\delta^2 T}{\delta z^2} + Q = \rho c \left[\frac{\delta T}{\delta t} - v \frac{\delta T}{\delta x} \right] \quad (2.1)$$

Together, the boundary conditions are summed up as in (2.2):

$$K_n - q + h(T - T_0) + \sigma \epsilon (T^4 - T_0^4) = 0 \quad (2.2)$$

When symmetric and insulation boundaries are considered as adiabatic, with no heat flowing through the surface, they are obtained by making convection zero and conduction zero from the surface, where, K_n is the thermal conductivity normal to the surface (W/mK), h is the convective heat transfer coefficient ($\text{W/m}^2 \text{K}$), ϵ is emissivity of surface radiating and σ is the Stefan Boltzmann's constant ($5.67 \times 10^{-8} \text{ W/m}^2 \text{K}^4$). When it is difficult to use radiation boundary condition, it is combined to convective heat flux by using a modified coefficient (h_r) for hot rolled steel plates with an error of about 5% as shown in equation (2.3)

$$h_r = 2.4 \times 10^{-3} \in T^{1.61} \quad (2.3)$$

Radiation inclusion will increase solution time by about three times and hence is combined with convection.

2.1. Peclet number definition and information

Peclet number gives thermal flow in liquid and from liquid to solid state. Peclet number at top surface of weld is $Pe(0)$ at $Z=0$

vertical distance and is $Pe(z)$ at any depth z . If the bead is conical or of frustum shape, as depth (d) increases, diameter of bead width (D) decreases. Peclet number is a function of weld width, weld speed (v), and thermal diffusivity (α) where, a is the radius of heat source power and m is an empirical multiplier as shown in equation (2.4)

$$pe(z) = pe(0) \left(1 - \frac{z}{d}\right) \text{ and } pe(0) = v * a/2 \quad (2.4)$$

Because of heat flow, the amount of power absorbed (P_l) in the inner side of weld is given as shown in equation (2.5)

$$P_l = t(m1 * Kmol) * (Tv - T0)(2.1995 + 3.1481Pe(0) - 0.16647Pe(0)^2 + 0.01152Pe(0)^3) \quad (2.5)$$

Here, t is the thickness of plate to be welded and $m1$ is empirical value to take care of variation in velocity and thermal conductivity. $Kmol$ is the thermal conductivity of molten metal, Tv is heat source temperature and $T0$ is initial temperature.

$p_t = p_c + p_l$ (2.6)
where p_t is the total power consisting of surface induced, p_c and p_l are from the melt metal laterally transferred to the solid base plate along with the thickness by conduction and in the presence of plasma key hole as given in equation (2.6).

In this study, different combinations of p_c and p_l are analyzed with the effects of temperature change and distortion and residual stresses that occur. The power calculated for different p_t are shown in figure A10. The variation of power for different bead temperatures is shown at different distances from the center of the weld.

2.2. Finite element for simulation

The heat equations can be represented in tensor form so that the elemental transient heat equation is obtained and then summed to get the system equation which is analysed with time as in equation (2.7)

$[K(T)]\{T\} + [C(T)]\{T\} = \{Q(T)\}$ (2.7)
where K is a temperature dependent conductivity matrix and C is the temperature dependent capacitance matrix based on specific heat, where their product with rate of temperature results in heat. The above equation

can be solved numerically, with standard FEM, Crank Nicholson or Euler time integration models. Assuming an initial temperature (T_i), K , C and Q are calculated at that temperature and the next temperature T , where $i+1$ is obtained. Again K , C and Q are calculated and temperature at next temperature interval is calculated. The iteration is continued for temperature convergence or heat flux values. This is a procedure for transient finite element analysis. In the present study, the work is done using Ansys.

2.3. Finite element model

The finite element model of dimensions 40mm x 150 mm x 5mm is used. AISI 304 austenitic stainless steel material is considered for simulations to be carried out. Convection is applied on all the surface of the plate except on the heat applied area. In this study, AISI type 304 stainless steel is used as it has many advantages such as low thermal conductivity, high resistance of corrosion and high stability at elevated temperatures. Thus SS304 material is widely used in numerous industries like nuclear industry, chemical plants, aeronautical and specialized pipe industries.

The properties of a typical stainless steel sheet and the temperature dependent thermal properties for AISI 304 stainless steel material are given in table1 and 2 respectively.

Table 1.Mechanical properties of AISI 304 Steel

Tensile strength	Yield strength	Density	Melting point	Thermal conductivity	% elongation
515 MPa	205 MPa	8000 kg/m ³	1400-1450°C	16.2 W/m°K at 100°C	20-40

Table 2.Temperature dependent thermal properties for AISI 304 Austenitic stainless steels

S.No	Temp (K)	Thermal conductivity, W/m °K	Density, Kg/m ³	Specific heat, J/Kg K
1	200	11	8200	350
2	400	15.5	8000	400
3	600	19	7800	440
4	800	22.5	7600	550
5	1000	26	7500	590
6	1200	30	7400	610
7	1400	34.5	7350	640
8	1600	39.5	7300	680
9	1800	44	7200	720
10	2000	47	7200	760

3. THERMAL ANALYSIS

Thermal analysis has been carried out with constant heat flux, where the thermal load is applied at a time on the weld area. Load is applied for first 10 sec and the temperature attains fusion in 40 seconds. The time step is progressively increased up to time=1000sec to see the plate cooling down to ambient temperature. In the present work, Finite Element Analysis (FEA) of single-pass butt-welding has been carried out with constant heat flux. A simple butt-joint welding whose welding parameters are consistent to those of Friedman's model with heat input $Q=2000\text{W}$ is considered and has been simulated using ANSYS. The present thermal Ansys is conducted using element type SOLID70. The element is applicable for three dimensional, steady-state or transient thermal analysis. The element can also compensate for mass transport heat flow from a constant velocity field. In this analysis, element SOLID70 is replaced by a three-dimensional (3-D) structural element SOLID45.

This element type has a three-dimensional thermal conduction capability and eight nodes with single degree freedom (temperature) at each node. The element is defined by eight nodes having three degrees of freedom at each node (translations in the nodal x, y and z directions). The element has plasticity, creep, swelling, stress stiffening, large deflection and large strain capabilities as depicted by ANSYS. The geometry and meshed model with tetrahedral shape with a volume mesh of size 0.02 were shown in figure A2. Figure A3 and A4 show the geometry (3mm thick) and mesh model used for analysis respectively.

[6-8] provides expressions and numerical models for different heat fluxes including Gaussian, where heat flux is in the shape of a normal distribution used for surface heat on fusion zone. Also, frustum is a part obtained by removing a part of the apex portion from a cone, where this distribution is used for keyhole heat. A combination of Gaussian on the surface and a conical heat distribution in the key hole is recommended for laser welding process as the bead ends in the thickness of the material. It was appropriate to use a conical heat flux distribution in the lateral surface of material. In case of EBW, though the heat flux distribution is same as EBW, the power of the beam makes the beam

open at the bottom of weld. This is better modeled by a frustum distribution of heat flux in the bead area or penetration area of the thickness of the plate instead of a cone. Here, the combination of Gaussian and frustum are used for heat flux model.

4. RESULTS AND DISCUSSION

Thermal results with heat flux values are obtained from Peclet number and used in EBW heat flux models. Mechanical properties of AISI 304 steel are shown in table 1. As temperature has an effect on both structural and thermal properties, its variation is incorporated in the analysis as shown in table 2. The variation of mechanical and thermal properties is incorporated in both thermal and structural analysis of the sequentially coupled procedure used.

The temperature distribution was found to be linear, as represented in figure A5. X axis is a ratio of surface to lateral heat and since the lateral heat is encompassed in the keyhole, convection in molten metal helps in fusion welding and excess heat is transferred to the wall and conducts freely.

The temperature distribution profile with color coding is shown in figure A6. For a 50:50 equal distribution of surface and lateral heat, the temperature at the base and the bead is about 470°K and 2586°K correspondingly. Similarly, in the 40:60 distribution of heat ratio of surface lateral heat, it is found to be 492°K and 2761°K respectively. In figure A7, the temperature change at bead variation with time is shown. It is shown for 30:70 ratio of surface to lateral heat, where the maximum temperature is 2800°K for about 40 seconds and after 1000 seconds it is 850°K.

4.1. Structural results

The structural results are shown for the power (30% Gaussian, 70% Frustum) distribution of the model. Due to the variance in the temperature gradient, the material properties are given in the model for elevated temperatures. A stress acting normal to the direction of weld bead is known as a transverse residual stress. Distortion is shown in figure A8, where the minimum distortion is at the base metal and the maximum distortion is at the weld bead is 0.2mm. The minimum V on Mises stress are at the base plate and the maximum Von Mises stress occurs at clamping points 305MPa, otherwise it is within 110MPa

at all other points as shown in the figure A9. The temperature near the weld bead and heat affected zone rapidly changes with distance from the heat source. This shows more stress value in the weld bead area and gradually decreases from center line to the base plate end. Both distortion and stresses are in acceptable limits in EBW.

5. CONCLUSIONS

An electron beam welding model using the keyhole formation and the Peclet number is discussed.

- The heat distribution is divided among the two: surface using Gaussian and Frustum distribution for lateral heat.
- A variation in the heat distribution is tried in which the surface to lateral heat equals from 50:50 to 30:70.
- A linearly increasing distribution with temperature getting better at bead with increase in lateral heat entrapped in keyhole is beneficial to obtain weld.
- Weld temperature would be obtained in about 40 seconds and rest of 1000 seconds would be for cooling down to ambient temperature.
- Distortions and stresses are stable with heat flux distribution changes and are well within the acceptable strength limits at 205MPa.

ACKNOWLEDGEMENT

The authors acknowledge the support from The Board of Research for Fusion Science and Technology (BRFST) for sanctioning the grant NFP-MAT-A11-02 and for creating simulation studies on welding processes for SS material under National Fusion Program.

REFERENCES

- [1] A.Kaplan, A Model of Deep Penetration Laser Welding Based on Calculation of the Keyhole Profile, *Journal of Physics D: Applied Physics*, Vol. 27, 1994, pp. 1805-1814.
- [2] R.Rai, T.A.Palmer, J.W.Elmer and T.Debroy, Heat Transfer and Fluid flow during Electron Beam Welding of 304L Stainless Steel Alloy, *Welding Research*, Vol. 88, No. 3, 2009, pp. 54-61.
- [3] C.H.Muralimohan, S.Haribabu, Y.Hariprasada Reddy, V.Muthupandi and K.Sivaprasad, Joining of AISI 1040 Steel to 6082-T6 Aluminium Alloy by Friction Welding, *Journal of Advances in Mechanical Engineering and Science*, Vol. 1, No. 1, 2015, pp. 57-64, <http://dx.doi.org/10.18831/james.in/20150110062455-0957>.
- [4] M.R.Frewin and D.A.Scott, Finite Element Model of Pulsed Laser Welding, *Welding Research Supplement*, Vol. 78, 1999, pp. 15-22.
- [5] Amudala Nata and Sekhar Babu, Finite Element Simulation of Hybrid Welding Process for Welding 304 Austenitic Stainless Steel Plate, *International Journal of Research in Engineering and Technology*, Vol. 1, No. 3, 2012, pp. 101-410.
- [6] T.Aseer Brabin and S.Ananth, Analysis of Overall Heat Transfer Coefficient and Effectiveness in Split Flow Heat Exchanger using Nano Fluids, *Journal of Advances in Mechanical Engineering and Science*, Vol. 1, Vol. 3, 2015, pp. 28-40, <http://dx.doi.org/10.18831/james.in/2015031004>.
- [7] P.Lucki and K.Adams, Numerical Simulation of the Electron Beam Welding Process, *Computers & Structures*, Vol. 89, No. 11, 2011, pp. 977-985, <http://dx.doi.org/10.1016/j.compstruc.2011.01.016>.
- [8] Suresh Akella, B.R.Kumar and V.Harinadh, Heat Flux for Welding Processes: Model for Laser Weld, *National Welding Seminar*, Bangalore, 2013.

APPENDIX

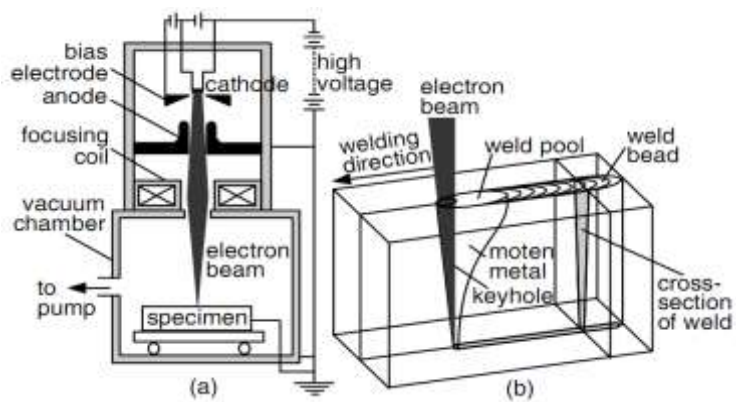
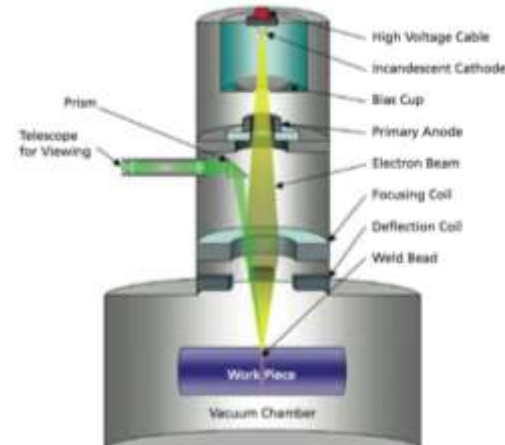


Figure A1. An electron welding beam generation equipment.

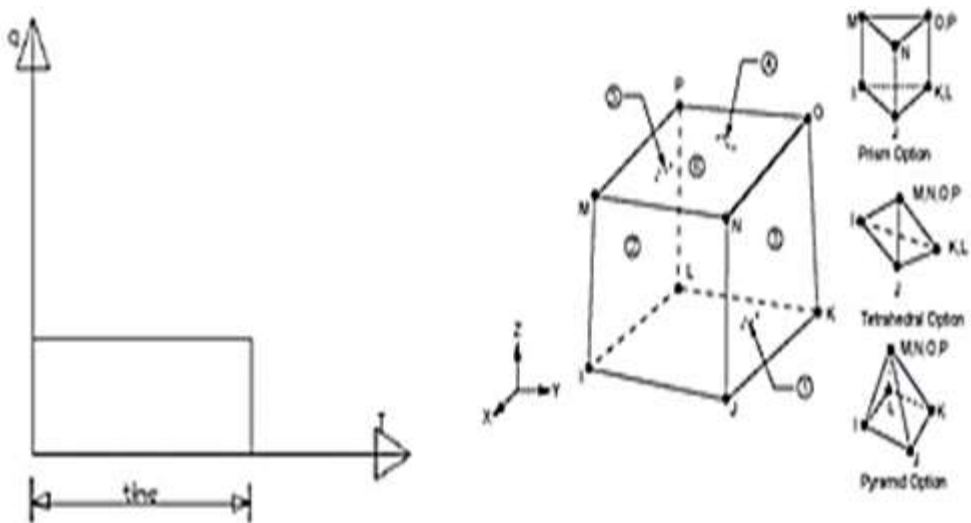


Figure A2. Mesh model used for analysis and element model used



Figure A3.Geometry of the model (3mm thick)

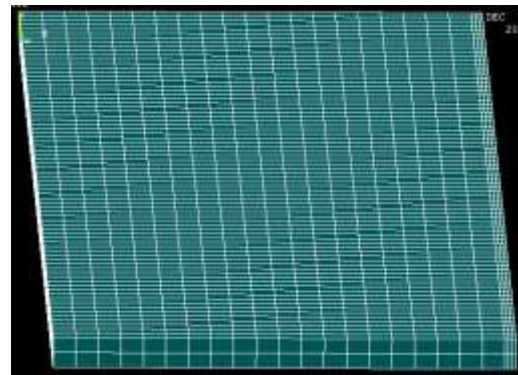


Figure A4.Mesh model used for analysis

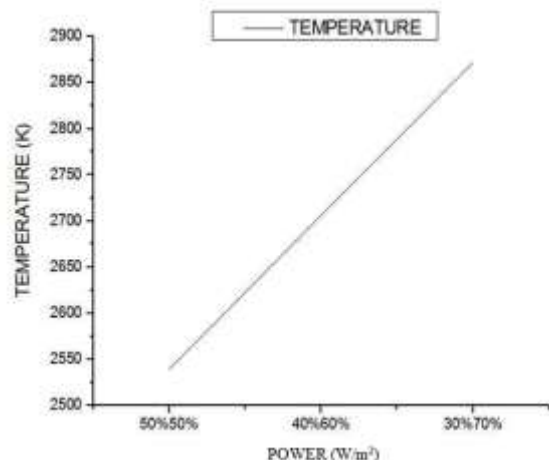


Figure A5.Power vs. temperature distribution

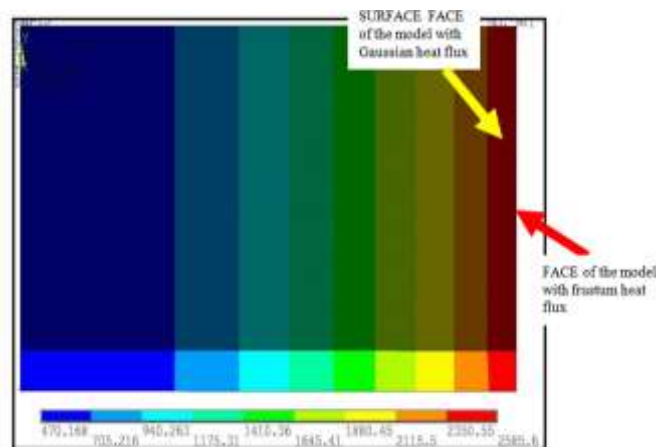


Figure A6.Temperature distribution of 50% Gaussian -50% Frustum

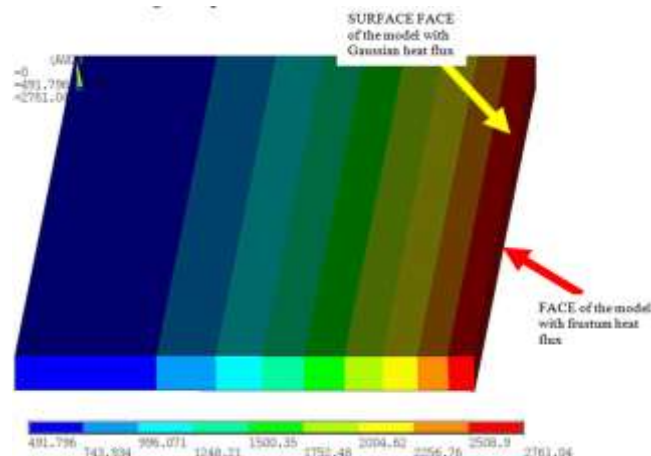


Figure A7a.Temperature distribution (40% Gaussian-60% Frustum of power)

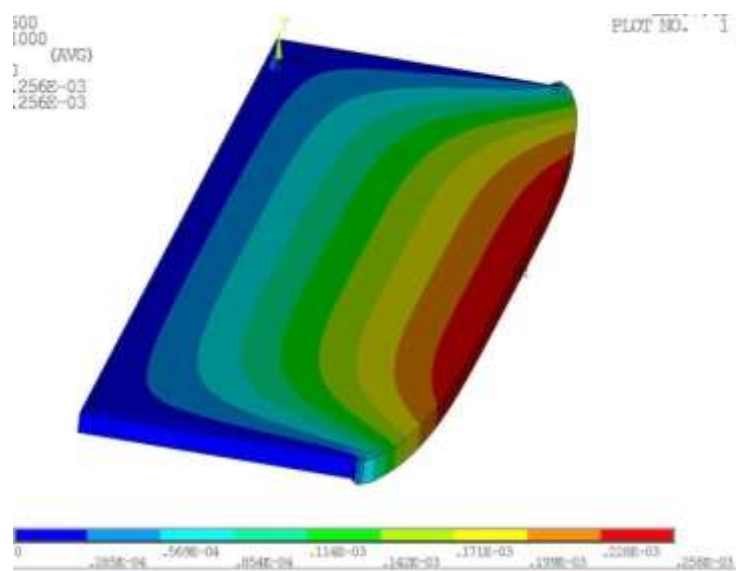


Figure A7b.Temperature distribution of 30% Gaussian -70% Frustum

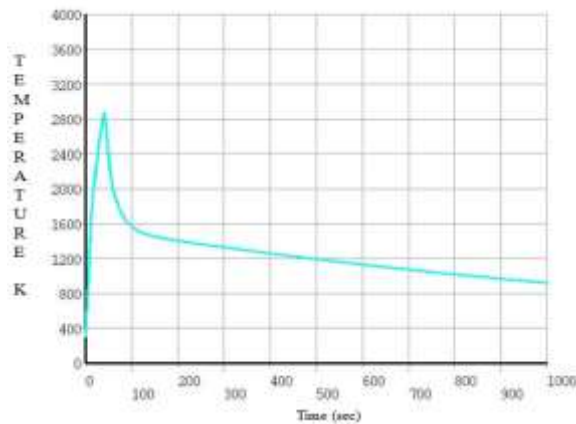


Figure A8.Distortion for 30% Gaussian – 70% Frustum

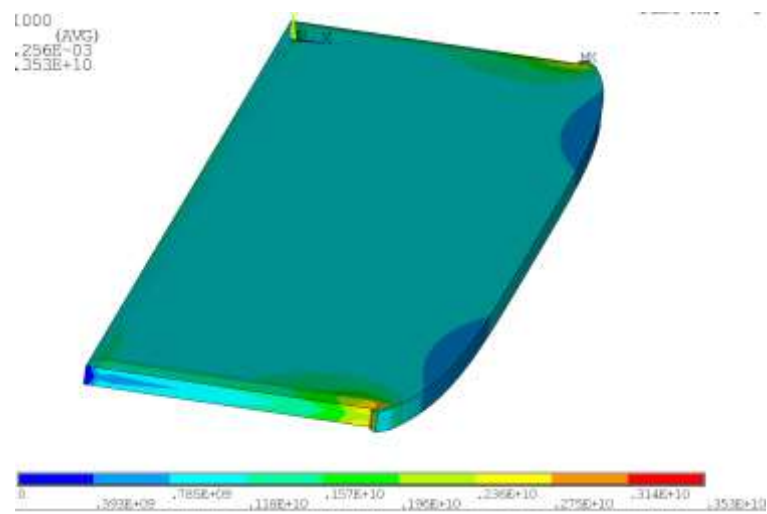


Figure A9.Von Mises stress for 30%Gaussian -70% frustum

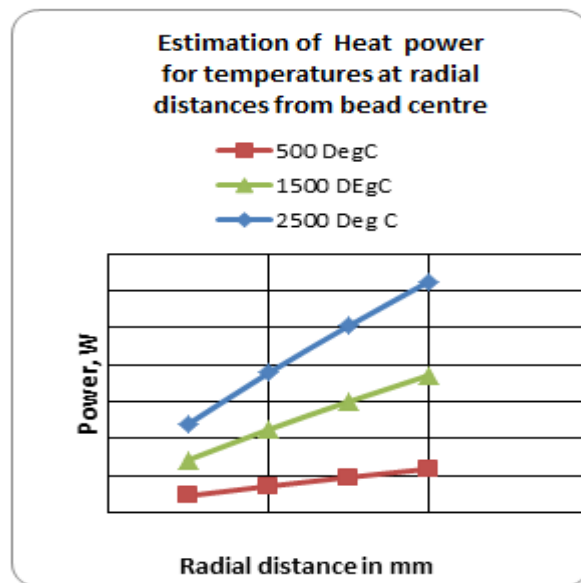


Figure A10.Power estimation using Peclet number